

CHAPTER 3

MATHEMATICAL MODELING OF THE DESALINATION PROCESS USING REVERSE OSMOSIS

3.1 INTRODUCTION

The last chapter elucidated the experimental setup and the factors influencing each unit of the large-scale seawater desalination process, with the reverse osmosis. This chapter deals with subjects such as the modeling of each unit of Sea water reverse osmosis (SWRO), the integration of these models to form an entire plant, and the future direction of the statistical modeling of the SWRO process. In order to model the SWRO process, a systematic understanding of each unit of the process is required. After investigating all the inputs and outputs of individual process units, the system models are formulated using the material balance continuity equations to predict the performance of each unit of the system. Synthesis is done to integrate the entire plant model to predict the permeate and brine characteristics from the RO membrane for the brackish/ sea water desalination process. The construction of the model for the large scale SWRO plant has the potential to reduce the cost of production of unit potable water(including both capital and maintenance/operating cost) so that it becomes a more attractive process for desalination than the others. These models will also be helpful in synthesizing the operational control strategies for producing (treatment) quality potable water under specified conditions. In this modeling investigation section, a review on the previous modeling of the

RO process is accomplished to develop the first principle equations for the designing and simulation of the SWRO process. Mathematical models have been developed using the first principle material balance and physical laws and are described in the following sections.

3.2 LITERATURE SURVEY (MODELING)

In literature, many models have been reported. Desalination using the RO technique came into vogue in the 1950s and was under research in the 1960s. In the next decade, the technology was subjected to commercialization. Models that adequately describe the performance of RO membranes are very important, since these are needed in the design of the RO processes. Models that predict the separation characteristics also minimize the number of experiments that must be performed to describe a particular system. Thus, a review on modeling techniques is given in the following section. The literature mainly gives an account of two types of phenomenological models of the desalination processes, namely, (i) the mechanistic model or membrane transport model and (ii) the lumped parameter model. Though there are distributed parameter models, we are interested in mostly mathematical models, that can be used directly in control applications. The former type can again be subdivided into three categories: irreversible thermodynamic models (such as Kedem-Katchalsky and Spiegler-Kedem models); nonporous or homogeneous membrane models (such as the solution-diffusion, solution-diffusion-imperfection, and extended solution-diffusion models); and pore models (such as the finely-porous, preferential sorption capillary flow, and surface force-pore flow models). The transport models focus on the top thin skin of asymmetric membranes or the top thin skin layer of composite membranes, since these determine the fluxes and the selectivities of most membranes. Most of these transport membrane models attain equilibrium in the membrane diffusion process, and describe the steady

state phenomena. The second type of models can describe the steady as well as transient behaviour that are required for control purposes. Murkes and Bohman (1972) developed a steady state model, relating the permeate flux to basic design parameters, to study the membrane performance under flow at different regions. The time domain dynamics help us to formulate laplace domain models around the operating point. Earlier reviews have been presented separately by many authors like Johnson (1980b), Soltanesh and Gill (1981), Mazid (1984), Pusch (1986b), Dickson (1988), Rautenbach and Albrecht (1989), and Bhattacharyya and Williams (1992c). The fundamental difference between the homogeneous and porous membrane models is the fact that the first assumes that, the membrane is nonporous and the transport of ions takes place through the interstitial spaces of the polymer chain by diffusion; whereas the porous model assumes that transport takes place through the pores along the membrane barrier layer by convection. Slater et al. (1985) presented a transient membrane mass transfer model for a small scale RO unit, using non-linear differential equations representing the feed conditions, flux, solute concentrations and rejections. Alatiqi et al. (1989) identified a MIMO transfer function model for the desalination process from the experimental data for closed-loop control. Transient models for membrane fouling phenomena were presented by Fountoukidis (1989), Jacob et al.(1996) and Hoek et al(2002). Davis and Leighton (1987) presented theories describing the transport of the concentrated boundary layer under laminar flow. Masahide and Shoji (2000) estimated the transport parameters of RO membranes for sea water desalination. The performance of RO systems was predicted by Riverol and Pilipovik (2005) using the feed forward neural network. Multi solute transport using 2-D mathematical model was explained by Ahmed et al.(2005) for the RO system. A dynamic model of membrane concentration polarisation using Nerst-Planck equation was suggested by Deon et al.(2007), and a film theory was developed by Chaaben and Andouls

(2008). All these models describe either the steady state mass transfer phenomena, or the transient dynamics of membrane concentration polarisation, and can be used to evaluate the process performance. In the case of sudden demand of potable water from a city (or with changes in the feed composition), the throughput has to be increased, that needs a transient model to predict the system performance and recovery ratios of the RO process. Thus, it was observed that there is a lack of modelling information that will directly help to construct the transfer function models for synthesizing controllers. Before we start developing the transient model for different units, let us review the status of different modeling of the RO and its development through the years.

3.2.1 Irreversible Thermodynamic Models

Irreversible thermodynamic models assume that the membrane is not far from equilibrium, and so fluxes can be described by phenomenological relationships. The water and solute fluxes are given by

$$K_W \left(\Delta P - (\pi_{Fc} - \pi_p) \right) = K_W \left((P_{Fc} - P_p) - (\pi_{Fc} - \pi_p) \right) \quad (3.1)$$

where K_w is the hydraulic permeability; suffix F is for feed, suffix $_{Fc}$ is for combined or mixed feed in the equalisation tank, suffix $_p$ is for the permeate, ΔP is for Applied Pressure and π is the osmotic pressure, and is given by Vant Hoff's relation as

$$\pi = \phi \left(\frac{n}{v} \right) R_g T \quad (3.2)$$

Where ϕ is the osmotic pressure coefficient

n is the number of moles of dissolved solute

v is the volume of the mixer

R_g is the gas constant

T is the temperature

Under isothermal condition, the above equation is reduced to

$$\pi = \beta.C \quad (3.3)$$

Where C is the molar concentration and

$$\beta = \phi R_g T \quad (3.4)$$

Similarly, for the solute side,

$$J_s = (\text{mass transfer rate of solute/membrane area}) = B_s \Delta C \quad (3.5)$$

Where B_s is the solute permeability constant, and ΔC is the concentration gradient of the solute across the membrane. Naturally, ΔC = difference in the concentration between the feed side and the permeate side. Pusch (1977) and Slater et al. (1985) derived the rejection ratio(R) as

$$R = 1 - \frac{C_P}{C_F} \quad (3.6)$$

The difficulty in the Kedem-Katchalsky (1958) model is that, the coefficient is dependent on the concentration, which was simplified by Spiegler and Kedem (1966), and thereby received wide applicability. But, the main defects of these models are that they are of the black box type (Dickson, 1988) and do not describe the membrane transport mechanism in

detail. In order to remove these difficulties Lonsdale et al. (1965) proposed a solution-diffusion model, based on the diffusion of the solute and the solvent through the membrane. The model assumes (Soltanieh and Gill, 1981; Bhattacharyya and Williams, 1992c) that (1) the RO membrane has a homogeneous, nonporous surface layer; (2) both the solute and solvent dissolve in this layer and then each diffuses across it; (3) the solute and solvent diffusion are uncoupled, and due to their own chemical potential gradient across the membrane; (4) and these gradients are the result of concentration and pressure differences across the membrane. Differences in the solubilities (partition coefficients) and diffusivities of the solute and solvent in the membrane phase are extremely important in this model, since they strongly influence the fluxes through the membrane. The solvent diffusion is given by Fick's law as

$$J_w = -D_{wm} \frac{dC_{wm}}{dz} \quad (3.7)$$

where D_{wm} is the diffusivity of the solvent and C_{wm} is the concentration of the solvent in the membrane, which is a function of the solvent's (water) chemical potential μ_w , and osmotic pressure is derived as

$$\pi = \frac{-R_g T}{V_w} \ln(a_w) \quad (3.8)$$

and the expressions of solvent flux as $J_w = A(\Delta P - \Delta \pi)$ (3.9)

and solute flux as $J_s = B(C_F - C_P)$ (3.10)

where A and B are constants. The principal advantage of the 'Solute Diffusion'(SD) model is that, only two parameters are needed to characterize the membrane system. As a result, it has been widely applied to both

inorganic salt and organic solute systems. However, Soltanieh and Gill (1981) indicated that the SD model is limited to membranes with low water content; Soltanieh and Gill (1981) and Mazid (1984) have also pointed out, that for many RO membranes and solutes, particularly organics, the SD model does not adequately describe water or solute flux. Thus, the imperfections in the membrane barrier layer, pore flow and solute-solvent membrane interactions, are taken into consideration by Sherwood et al. (1967). Imperfections or defects (pores) on the surface of the membranes, through which transport can occur, were brought to notice and better models were formulated. The total water flux through the membrane is expressed as

$$N_w = J_w + K_2 \Delta P \quad (3.11)$$

Similarly, the solute flux is $N_s = J_s + K_2 \Delta P$ (3.12)

where K_2 is a constant

Though this fits the experimental data excellently, it has two major disadvantages: it contains three parameters that must be determined by nonlinear regression in order to characterize the membrane system; and the parameters describing the system are usually functions of both the feed concentration and pressure (Soltanieh and Gill, 1981). Also, some dilute organic systems ($\theta = \pi \Delta$) have substantially lower water fluxes than those predicted by N_w . Burghoff et al. (1988) pointed out that the solute-diffusion model does not explain the negative solute rejection in the case of some organics, and presented a revised model that takes care of the possible pressure dependence of the solute chemical potential, that has a negligible effect on inorganic solutes, but contributes to organic solutes. The chemical potential is given by

$$\mu_s = R_g T \ln \left(\frac{C_F}{C_P} \right) + V_s \Delta P \quad (3.13)$$

which can be rewritten in terms of the solute flux as

$$J_s = \frac{D_{sm} K_{sm}}{\delta} (C_F - C_P) + L_{sp} \Delta P \quad (3.14)$$

where δ is the thickness of the membrane, D_{sm} is the diffusion coefficient and K_{sm} is the distribution coefficient of the solute, L_{sp} is a parameter responsible for the transport, due to the pressure difference across the membrane. In doing so, Burghoff et al.(1980) found that the model adequately describes the transport of some organic solutes, but it still does not address the substantial decreases in the water flux found in some dilute organic systems, and hence, is not widely used in practice.

All the above ambiguities were successfully solved by the pore diffusion model that was presented by Sourirajan (1970). This model assumes that the membrane is micro porous (capillary structure), for the first time in the history of transport through membrane processes, and the mechanism of separation is determined by both the surface phenomena and fluid transport through pores in the RO membrane. The authors state that the barrier layer of the membrane has a chemical property, by which it absorbs the solvent preferentially and repels the solute of the feed solution. The water flux accordingly is given by

$$J_w = A \left(\Delta P - \left(\pi(X_f) - \pi(X_p) \right) \right) \quad (3.15)$$

where A is the permeability constant and $\pi(X)$ represents the osmotic pressure at the solute mole fraction X . Similarly the solute flux is given by

$$J_s = \frac{D_{sp} K_D C_T}{\delta} (X_f - X_p) \quad (3.16)$$

where K_D is the distribution coefficient. Sourirajan and Matsuura (1985) used this model widely to analyze the transport of a large amount of the solute through the membrane but, it fails to explain the drop in the water flux caused by some dilute organic solutes and the rejection behavior of some solutes. These problems were solved by assuming the membranes to be finely micro porous in nature by Merten (1966), and separately by Johnson and Boesen (1975). This model assumes that the transport of the solvent is caused by the viscous flow through uniform membrane pores, and the transport of the solute is by diffusion as well as convection processes. Soltanieh and Gill, (1981); Sourirajan and Matsuura, (1985) assumed that membranes are of length $\tau\delta$ and of radius R_p and derived that the solute flux is

$$J_s^{Pore} = \frac{-R_g T}{X_{sw} b} \frac{dC_{pore}}{dz} + \frac{uC_{pore}}{b} \quad (3.17)$$

where $b = \frac{X_{sw} + X_{sm}}{X_{sw}} = \frac{D_{sw}}{D_{sm}}$ and u is the velocity of the solute through the pores. The parameter b is defined as the ratio of the frictional force acting on the solute moving in a membrane pore to the frictional force experienced by the solute in a free solution. The solvent (water) transport mechanism is established by balancing the effective pressure driving force with the frictional force between the solute and pore wall; accordingly, the solvent flux is given by

$$J_w = \varepsilon u = \frac{\varepsilon R_p^2 \Delta P}{8\eta \tau \delta} \left[\frac{1}{1 + \frac{R_p^2 X_{sm} C_p}{8\eta}} \right] \quad (3.18)$$

where ε is the porosity and X_{sm} is the frictional force between the solute and the membrane. Jonsson and Boesen (1975); Soltanieh and Gill (1981); Dickson (1988), used this model and showed that it is able to provide valuable insight regarding parameters such as the solute-membrane interaction (friction), solute distribution coefficient and pore size. They successfully explained the transport process of the solute through the membrane using this finely porous model. However, this model is not adequate to account for the decreases in the water flux compared to the pure water flux, unless a correction is made in the pore size, for the measured and predicted water flux to agree. The disadvantage of this model is that it can only be used for the water flux correctly. This inconsistency was modified by Mehdizadeh and Dickson (1990) by reducing the pore sizes, and by introducing a term on the diffusive component of the flux at the pore outlet. He presented the equation for predicting the permeate concentration as

$$C_p = C_F - (C_p - C_F) \left[\frac{1 - \exp\left(\frac{uX_{sw}z}{R_g T}\right)}{1 - \exp\left(\frac{u\tau\delta X_{sw}}{R_g T}\right)} \right] \quad (3.19)$$

This can be solved by the trial and error method. An Analytical solution is possible by introducing the boundary condition on the pore size. Zadeh compared his model with the original finely-porous model, using the same parameters, and found that the predicted permeate concentration of the modified finely-porous model was always higher than that of the original finely-porous model. The finely-porous model needs separation process data for the evaluation of some transport process parameters, and the comparative performance studies of these models are unavailable.

Later on, Matsuura and Sourirajan, (1981), Sourirajan and Matsuura, (1985) and Dickson (1988) modified their finely porous model (that assumed only the axial distribution of the solute) by extending the solute concentration through a RO membrane pore in the axial as well as in the radial directions. They named it the surface force-pore flow model which assumes (1) that water transport through the membrane occurs in the pores by the viscous flow; (2) the solute transport takes place by diffusion and convection in the membrane pores; (3) transport of both the water and solute through the membrane pores is determined by interaction forces, friction forces, and chemical potential gradients of the water and solute; (4) the pores of the membrane are cylindrical and run the length of the membrane barrier layer; (5) a molecular layer of pure water is preferentially absorbed by the pore wall; and (6) a potential field controls the solute distribution of the membrane pore. They formulated the following model

$$\begin{aligned} \frac{d^2u}{dr^2} + \frac{1}{r} \frac{du}{dr} + \frac{1}{\eta} \frac{R_g T}{\delta} (C_p(r)|_{z=\delta} - C_F) \left[1 - \exp\left(\frac{\Phi(r)}{R_g T}\right) \right] \\ - \frac{1}{\eta} [b(r) - 1] X_{sw} C_p(r)|_{z=\delta} u = 0 \end{aligned} \quad (3.20)$$

with boundary condition $\frac{du}{dr}|_{r=0} = 0$ and $u(R) = 0$

Assuming the water flow by the Poiseuille equation, the water flux is given by

$$\frac{J_w}{J_{w0}} = \frac{2 \int_0^{R_F} u \, r \, dr}{R_p^4 \Delta P} \quad (3.21)$$

and the force balance on the solute around the pores gives the formula to predict the permeate concentration at the pore outlet

$$\frac{C_p(r)|_{z=\delta}}{C_F} = \frac{\exp\left(u(r)\delta \frac{X_{Sw}}{R_g T}\right)}{1 + \frac{b(r)}{\exp\left(\frac{-\Phi(r)}{R_g T}\right)} \left[\exp\left(u(r)\delta \frac{X_{Sw}}{R_g T}\right) - 1 \right]} \quad (3.22)$$

The boundary conditions are given by the Maxwell Boltzman distribution law:

$$C_{Pore}(r, 0) = C_F \exp\left(\frac{-\Phi(r)}{R_g T}\right) = K_D(r) C_F \quad (3.23)$$

and

$$C_{Pore}(r, \delta) = C_p(r)|_{z=\delta} \exp\left(\frac{-\Phi(r)}{R_g T}\right) = K_D(r) C_p(r)|_{z=\delta} \quad (3.24)$$

where $\phi(r)$ is the coulombic potential function, and is represented by

$$\Phi(r) = \frac{A'}{R_p - r}$$

and A' is the measure of the electrostatic repulsion force between the ionic solute and the membrane. The modification of this model brought by Sourirajan & Matsurra (1985) was through the inclusion of the realistic data of pore size distribution. But in spite of these modifications, there still exists some inconsistencies with the separation of some solutes and hence, it is not obvious that these models provide better solute separation predictions.

Another group of researchers started using charged RO membrane theories for predicting the ionic solute separations. Bhattacharyya and Williams, (1992c) stated that when a charged membrane is placed in a salt

solution, dynamic equilibrium is established. The counter-ion of the solution, opposite in charge to the fixed membrane charge (COOH^- or SO_3^- radicals), is present in the membrane at a higher concentration than that of the co-ion (same charge as the fixed membrane charge) because of electrostatic attraction and repulsion effects. This creates a Donnan potential, which prevents the diffusive exchange of the counter-ion and the co-ion between the solution and the membrane phase. When a pressure driving force is applied to force water through the charged membrane, the effect of the Donnan potential is to repel the co-ion from the membrane; since electro neutrality must be maintained in the solution phase, the counter-ion is also rejected, resulting in ionic solute separation. The model was named as the charged membrane model. Garcia and Medina (1989) reported some success in the use of the dimensional analysis to correlate the experimental RO membrane data. Mason and Lonsdale (1990) presented the general statistical-mechanical theory of membrane transport; they pointed out that most RO membrane transport models (solution-diffusion, diffusion-convection, etc.) could be derived from the statistical-mechanical theory. Bitter (1991) also developed a general model based on the solution-diffusion mechanism, using Maxwell-Stefan equations to calculate diffusive transport, and Flory-Huggins equations to calculate the solubility of the species in the membrane. Many other researchers, Deshmukh (1989), Rautenbach and Gröschl (1990a, 1991), Kothari (1991), and Kulkarni et al. (1992) etc; used empirical correlations and formulated models to predict the membrane transport processes.

3.2.2 Concentration Polarization

Generally, part of the rejected solute adheres on the surface of the membrane and slowly builds up a boundary layer, in which the concentration of the solute is more than that of the solute at the centre of the membrane tube, where the flow is turbulent. As water passes through the membrane, the

convective flow of the solute to the membrane surface is much larger than the diffusion of the solute back to the bulk feed solution; as a result, the concentration of the solute at the membrane wall increases. This is known as concentration polarization. Matthiasson and Sivik (1980), Gekas and Hallstrom (1987), Rautenbach and Albrecht (1989), and Bhattacharyya and Williams (1992c) have reported their studies on this area in detail. Due to the development of concentration polarization, (1) there is an increase in the solute flux through the membrane because of an increased concentration gradient across the membrane (2) there is a decrease in the water flux due to increased osmotic pressure at the membrane wall (3) there is an exhibition of changed membrane separation properties (4) there is a precipitation of the solute if the surface concentration exceeds its solubility limit, leading to scaling or particle fouling of the membrane and reduced water flux and (5) particulate or colloidal materials in the feed start blocking the membrane surface, that reduces the water flux and enhances membrane fouling. These effects can be reduced by greater mixing of the solutes in the stream inside the membrane, that can be done by slowly increasing the pressure of the pump. Let us assume that a solute with bulk feed concentration (C_F) enters the RO system, and builds up a concentration polarization layer with the solute concentration (C_W). In the case of very high feed flow rates, there is good mixing inside the stream that makes C_W almost equal to C_F , by reducing the thickness [$\xi(z)$] of the boundary wall to almost zero. This concentration profile due to the diffusion–convection phenomenon for the flow over a flat sheet membrane, can be described by a Navier Stroke Equation as

$$U \frac{\partial C}{\partial z} + V \frac{\partial C}{\partial y} - D_{sw} \left(\frac{\partial^2 C}{\partial z^2} + \frac{\partial^2 C}{\partial y^2} \right) = 0 \quad (3.25)$$

with boundary conditions

$$C(0, y) = C_F \quad \text{and} \quad \frac{\partial C(z, 0)}{\partial y} = 0 \quad ; \quad D_{sw} \frac{\partial C[z, \xi(z)]}{\partial y} = V_w \{C[z, \xi(z)] - C_P(z)\} \quad ;$$

$$C[z, \xi(z)] = C_w(z) = \frac{C_P(z)}{1-R} \quad \text{with } R \text{ as rejection}$$

A simple case may be thought of when the boundary layer is stagnant, and does not change with the membrane's length; i.e., $\xi(z) = \xi$ then the above PDE reduces to

$$V_w \frac{\partial C}{\partial y} = D_{sw} \frac{\partial^2 C}{\partial y^2} \quad (3.26)$$

That can have an analytical solution (Bhattacharyya and Williams, 1992c).

$$\frac{C_w - C_P}{C_F - C_P} = \exp\left(\frac{V_w \xi}{D_{sw}}\right) \quad (3.27)$$

Kim and Hoek (2005) modeled the concentration polarization numerically to enable the local description of the permeate flux and solute rejection in cross flow reverse osmosis separations. Predictions of the channel averaged water flux and salt rejection by the developed numerical model, the classical film theory model, and analytical models available in literature, were compared with those of well-controlled laboratory scale experimental data. Masaaki (1996) proposed a friction-concentration-polarization model that used the Kimura-Sourirajan model for the transport phenomenon of the solute and water transport through a membrane, taking a mass transfer coeff. as the local variable and taking a fiber-bore side pressure drop into account. Marinas and Urama (1996); Bouchand, and Lebran (1999) studied the effect of the feed flow on concentration polarization, and modeled it on the RO spiral-wound element. Murthy and Gupta (1997) estimated the mass transfer

coefficient, K , by (a) direct measurements, using optical or microelectrode measurements; (b) indirect measurements, in which the true rejection is calculated by extrapolation to infinite feed circulation; and (c) indirect measurements, in which a conc. polarization model combined with a membrane transport model is used for the mass transfer coeff. calculation. They suggested that the Spiegler-Kedem film theory may be the best method for estimation, and the related Sherwood number with K . Chen (1998) also found that at low wall concentration, fouling increases.

Various factors affecting the RO process are categorized under the feed variables (solute concentration, temperature, pH, and pretreatment requirements), the Membrane variables (polymer type, module geometry, and module arrangement), and the process variables (feed flow rate, operating pressure, operating time, and water recovery). Experiments have shown that generally, the solute flux increases with applied pressure as well as with temperature since the solute (water) diffusivity increases, and the viscosity decreases with temperature. With an increase in the feed solute concentration, the solute flux decreases as it results in large osmotic pressure. Solute rejection increases with pressure since the water flux through the membrane increases, while the solute flux is essentially unchanged when the pressure is increased. In the case of some organics, rejection decreases with pressure, due to strong solute-membrane interactions. An increase in the temperature keeps the rejection of the solute almost constant, or shows a decreasing trend. The feed pH generally does not affect the solvent flux or solute rejection. The feed solvent (water) quality is important for the long life of the membrane quality and for avoiding fouling that needs pretreatment. Other than polarization, nanofiltration through membranes was discussed by a number of authors (Labbez et al. 2002, Muhammed et al. 2007, Deon et al., 2007, Scymczyk, 2009 & 2010). The ultrafiltration of electrolytes was presented by Yaroschuck (2008); Pontie et al. (2008) and Sarrade et al (1994).

The above study gives the art of steady state and concentration polarization models in RO units. Though a few dynamic models are available, they are either complex in structure or need more computational time. This indicates that there is a lack of simple dynamic models that can be used for analyzing and synthesizing operational safety and control strategies. Hence, in the present work, a dynamic model for a RO desalination unit is presented. A simple schematic of an RO process is presented in Figure 3.1 for formulation of modeling. Raw water is pre-treated and stored temporarily in an equalisation tank, from which it is pumped using high pressure to the membrane chamber, to overcome the osmotic pressure barrier that causes the solvent (potable water) to transport from the feed to the permeate side. The performance of the process depends on the pressure, temperature and concentration of the dissolved solids. For the stable operation of the RO processes, an analysis of these membrane processes, using a mathematical model, is necessary to improve the plant performance, its efficiency, safety and reliability.

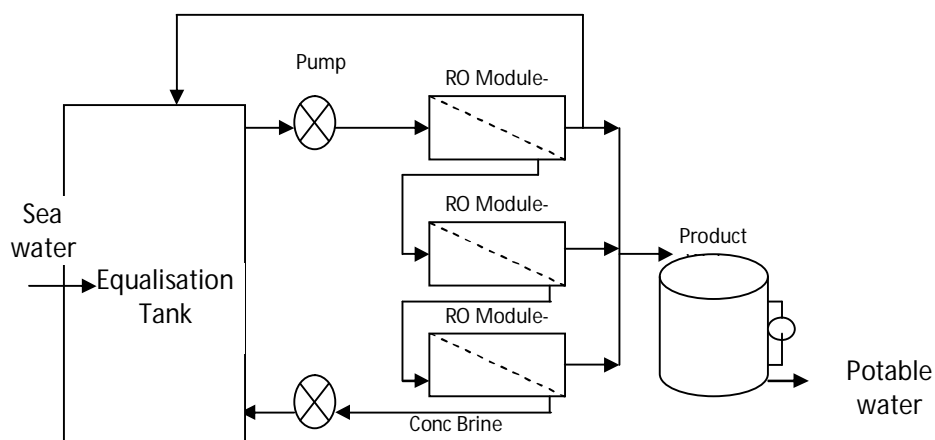


Figure 3. 1 Schematic of a typical reverse osmosis desalination process

Naturally, the measured variables in the process are the flow rate and the concentration of the dissolved solids in product water; the manipulated variable is the pressure on the feed water side, and the load is the flow rate of the feed water as it varies according to demand. The objective of this chapter is to formulate a simplified steady state mass transfer model and to develop transient dynamics of concentration polarisation for the construction of a simple control strategy for this process.

3.3 DEVELOPMENT OF MASS TRANSFER MODEL

The permeate (p) (due to the radial component of velocity) comes out along the surface of the membrane, while the concentrated brine (due to the axial component of velocity) flows axially through the membrane. The RO process can be thought of as comprising a grey box model (Figure 2.8) with one input or manipulated variable, several disturbance & design variables, and output or control variables. Models that predict the separation characteristics also minimize the number of experiments that must be performed to describe a particular system. Models that adequately describe the performance of the RO membranes are very important, since these are needed in the design of the RO processes. Due to the transverse diffusion across the walls of RO tubes (cylindrical), the permeate comes out and gets accumulated in the product tank. The axial flow stream goes out as rejection or brine.

3.3.1 Basic Mass Transfer Steady State Model

This model assumes that the membrane tubes are arranged in a single stack in parallel, to constitute a module. Raw feed enters at the flow rate Q_{f0} and a solute concentration C_{f0} that mixes in the equalisation tank. Recycle streams of the permeate and the retentate also enter this tank

resulting in a mixed feed (c) with a concentration of C_f that is pumped (with a pressure P_f) to the RO module. Thus, there are two velocity components (one is axial and the other acts radial along the membrane axis) of the feed stream.

The permeate (p) (due to the radial component of velocity) flows through the surface of the membrane, while the concentrated brine (due to the axial component of velocity) flows axially through the membrane. The steady state model helps us to calculate the variables associated with each stream at the exit of each equipment/unit. It is evident from Figure 3.1 that there are mostly four units: the mixing, RO, permeate and brine tanks. The equations for each unit can be developed thus.

3.3.1.1 Permeate stream

The permeate flux is given by

$$J_w = K_w (\Delta P - (\pi_{mT} - \pi_p)) = K_w ((P_{mT} - P_p) - (\pi_{mT} - \pi_p)) \quad (3.28)$$

where K_w is the hydraulic permeability or water mass transfer coefficient; suffix F is for feed, mT is for the combined or mixed feed in the equalisation tank, P is for pressure, p stands for the permeate and π is the osmotic pressure and is given by

$$\text{Vant Hoff's relation as } \pi = \phi \left(\frac{n}{v} \right) R_s T \quad (3.29)$$

where ϕ is the osmotic pressure coefficient

n is the number of moles of dissolved solute

v is the volume of the mixer

R_g is the gas constant

T is the temperature

Under isothermal conditions, the above equation is reduced to

$$\pi = \beta.C \quad (3.30)$$

where C is the molar concentration and $\beta = \phi R_g T$.

The Concentration of the permeate (C_p) can be found from Equation (3.30).

As the impermeable solutes accumulate inside the membrane surface, a laminar boundary layer is formulated for which the concentration polarization is given by

$$\frac{C_{mT} - C_P}{C_b - C_P} = \exp\left(\frac{J_W}{K_{CP}}\right) = \alpha \quad (3.31)$$

where C_b is the bulk phase concentration, and K_{CP} is the concentration polarization mass transfer coefficient, given by (Hyun-Jeoh et al.2009)

$$K_{CP} = \frac{0.023 C_{mT} N_{Re}^{0.83} N_{Sc}^{0.33}}{2L} \quad (3.32)$$

With Reynolds number $N_{Re} = \frac{\rho d_m u}{\mu}$ and Schmidt number $N_{Sc} = \frac{\mu}{\rho D_L}$ where

d_m = diameter of RO membrane, D_L is the liquid diffusivity, μ is the viscosity of liquid and u = liquid velocity, L =length of RO tube and ρ = liquid density.

Thus the volumetric flux, in Eqn. (3.28), can be rewritten as

$$J_w = K_w ((P_{mT} - P_p) - \beta(C_{mT} - C_p)) = K_w ((P_{mT} - P_p) - \beta\alpha(C_b - C_p)) \quad (3.33)$$

where C_B is the bulk liquid concentration inside the membrane and can be calculated as

$$C_B = \frac{C_{mT} + C_b}{2} \quad (3.34)$$

with C_{mT} as the feed concentration and C_b as the concentration of the retentate (brine) at the exit of the RO module.

3.3.1.2 Mixing Tank

Equation (3.28) may be used to obtain the permeate flux (J_w). Equation (3.33) is then applied to get the permeate concentration (C_p). With this value of C_p , the bulk concentration of liquid, C_B can be calculated using Equation (3.31). The retentate concentration (C_b) can be found from Equation (3.34).

$$\text{Permeate flow can be related as } F_p = J_w S_a \quad (3.35)$$

where $S_a = W(dz) = \frac{a}{L} dz$ = surface area of membrane. where a =area, L =length along RO, z =thickness of RO, W =width of RO. Empirical relation has been used to calculate S_a by Bouchard and Lebrun (1999).

The combined flow is given by Sobana and Panda(2013)

$$F_{mT} = F_F + (1 - p)F_p + bF_b \quad (3.36)$$

where $1-p$ = fractional flow of the permeate added to the equalisation tank($p=1$) and

b = fractional flow of the retentate added to the equalisation tank.

3.3.1.3 Brine Tank

To calculate the brine flux the following equation can be used by

$$J_b = K_s \beta (C_{mT} - C_P) \quad (3.37)$$

$$\text{Thus } F_b = J_b S_a \quad (3.38)$$

with this value of F_b , The flow rate of the combined feed stream can be calculated using Equation (3.36). Osmotic pressure is a function of temperature and concentration. Osmotic pressure can be calculated by $\pi = (0.6955 + 0.0025T) \times 10^8 \times \frac{C_i}{\rho_i}$ where C_i is the concentration (ppm) and ρ is the density (kg/m^3) at the interface at temperature $T^\circ\text{C}$. The density can be given by $\rho = 498.4m + \sqrt{(248400m^2 + 752.4mC)}$ where the constant m is given by $m = 1.0069 - 2.757 \times 10^{-4}T$. The Salt concentration (C) at the membrane wall is $C_i = C_P + (C_{Fc} - C_P) \times \exp\left(\frac{J_w}{K_s} \times 1000\right)$. The mass transfer coefficient $K_s = 1.101 \times 10^{-4} u_b^{0.5}$, where u_b is the velocity (m/s) of the brine and C_{FC} is the concentration of the combined feed (feed + brine).

3.3.1.4 RO section

Thus the volumetric permeate flux is $J_P = J_w / \rho_P = K_w ((P_{Fc} - P_P) - \beta \alpha (C_B - C_P)) / \rho_P$. With the development of the cake layer on the membrane, the permeate flux is given by (Hyun-Jeoh et al.2009),

$J_w = \frac{\Delta P - \Delta \pi}{\mu(R_m + R_c)}$ where R_m is the membrane resistance, and R_c is the resistance imparted by the cake layer deposited over the membrane surface, and is given by $R_c = \alpha M_d = \left[\frac{45(1-\varepsilon)}{\rho_c a_p^2 \varepsilon^3} \right] M_d$ where ρ_c is particle cake density, and a_p is the particle radius and M_d is the mass deposition rate of the cake given by (Pakkonen et al.1990), $M_d = \frac{\rho_c dx_c}{dt}$ where ρ_c is the density of the cake and dx_c/dt is the rate of change of cake thickness. $\mu = \frac{\eta}{\rho}$, with η as the viscosity and ρ as the density of the fluid. The Cake layer can be calculated from $\delta_c = \left[\frac{(4/3)\pi a_p^3}{1-\varepsilon} \right] M_c$ where M_c is the total number of particles per unit area, accumulated in the cake layer. At pH = 7.1, $M_c = 8.56 \text{ g/m}^2$, $\alpha = 2.71 \times 10^{-15} \text{ m/kg}$ and $\delta_c = 20$ for sea water.

Mindler and Epstein (1986) approximated C_{CW} (concentration at the interface of the cake and the liquid) with the following relation $\frac{C_{CW}}{C_B} = 1.33 \exp\left(\frac{\gamma}{0.75 \delta} y\right) C_p$ with $\gamma = \frac{2V_{mT}(N_{SC})^{2/3}}{fu_x}$ and f as the friction factor for turbulent flow (Min et.al, 1984). y is the radial distance, δ is the thickness of the concentration polarization, V_{mT} Volume of mixing tank and u_x is the velocity in axial direction. Equation (3.31) can be solved to get the concentration profile along the RO membranes (i.e) concentration of bulk stream(C_b) inside the membrane can be found. .

3.3.2 Transient Model

The system considered here consists of an equalisation feed tank, an RO membrane module and a product collection tank. The Feed enters the membrane module through a feeding pump and a part (b) of the concentrated

brine that comes out (axially) from the RO is recycled to the equalisation tank. Similarly, a part of the permeate (1-p) (radially) that comes out through the membrane gets recycled to the equalisation tank. After developing the steady state balance equations, one needs to formulate the transient dynamics around the tanks and RO module, to design a safe and efficient control of the system. The transient dynamics are derived as follows:

3.3.2.1 Feed / Equalisation Tank

The transient mass balance equation given by Sobana and Panda (2013) around the mixing tank becomes

$$V_{mT} \frac{dC_{mT}}{dt} = \dot{M}_{so} + b\dot{M}_{bo} + (1-p)\dot{M}_{po} - \dot{M}_{mm} \quad (3.39)$$

where dots on top of variables represent mass flow rates;

with initial conditions as:

$$\begin{aligned} &\text{at } t=0, V_{mT} = V_{so} \\ &\text{and} \\ &C_{mT} = \left[\frac{F_{so} + bF_{bo} + (1-p)F_{po}}{F_{mm}} \right] \end{aligned} \quad (3.40)$$

If we want to maintain a constant holdup in the equalisation tank, assume, $V_{mT} = \text{constant}$,

The Laplace transformed continuity equation of the integrated system becomes

$$C_{mT}(s) = \frac{F_{so}C_{so}(s)}{sV_{mT} + F_{mm}} + \frac{bF_{bo}C_{bo}(s)}{sV_{mT} + F_{mm}} + \frac{[1-p]F_{po}C_{po}(s)}{sV_{mT} + F_{mm}} \quad (3.41)$$

Three streams (sea water, the exit stream from the brine tank and the exit flow from the permeate tank) are considered to enter the mixing tank, from which a single stream goes out as the mixed flow. The Volumetric flow rates of the streams are F_{so} , F_{bo} and F_{po} in m^3/hr . Similarly, the height (h_{mt}) of the liquid is related to inlet flow rates around the mixing tank as

$$h_{mT}(s) = \frac{C_{so}R_{mT}/C_{mm}}{R_{mT}A_{mT}^{s+1}}F_{so}(s) + \frac{C_{bo}R_{mT}/C_{mm}}{R_{mT}A_{mT}^{s+1}}F_{bo}(s) + \frac{C_{po}R_{mT}/C_{mm}}{R_{mT}A_{mT}^{s+1}}[1-p]F_{pd}(s) \quad (3.42)$$

where s is the Laplace variable.

3.3.2.2 Membrane module

(Concentration Polarisation)

Concentration polarisation (Michael, (1988)) Fluid transport through the horizontal porous membrane (of length L and radius r) is assumed to have axial (u_x or horizontal) and radial (u_y or vertical) components of velocity. The radial component gives rise to the permeate flow. The concentration polarisation that is developed due to the separation of the boundary layer is given by

$$\frac{\partial C}{\partial t} = D_L \frac{\partial^2 C}{\partial y^2} - u_y \frac{\partial C}{\partial y} - u_x \frac{\partial C}{\partial x} \quad (3.43)$$

with initial conditions: $C=0$ at $t=0$ and

$$\frac{\partial C}{\partial y} = 0, \text{ at } y=0 \quad (3.44)$$

and boundary conditions: $C=C_0$ at $x=0$, and

$$D_L \frac{\partial C}{\partial y} = u_y C - V_p C_p \text{ at } y=R \quad (3.45)$$

The solution of the above PDE equations (3.43) becomes

$$C = \frac{2}{L} \sum_{n=1}^{\infty} \sin\left(\frac{n\pi y}{L}\right) \sin\left(\frac{n\pi x}{L}\right) e^{-k^2 D_L U t} \quad (3.46)$$

where $U = \sqrt{u_x^2 + u_y^2}$ and $u_y = \frac{\nabla P}{2\eta L} (4R^2 - y^2)$ and $u_x = u_m \left(\frac{R^2 - x^2}{R^2} \right)$ and

$\kappa^2 = \frac{dy^2}{y} \left(\frac{n\pi}{L} \right)^2 = \text{constant} (\approx 0.1, 0.2, \dots, 1.0)$. ∇P is the applied pressure, u_m is the

fluid velocity at the centre of the membrane tube. Permeate flux J_w is given by

$$J_w = K_w \left[(P_{mT} - P_p) - \beta (C_{mT} - C_p) \right] \quad (3.47)$$

Differentiating (w. r. to t) the above equation,

$$\frac{dJ_w}{dt} = K_w \left[\frac{d\Delta P}{dt} - \beta \frac{dC_{mT}}{dt} \right] \quad (3.48)$$

Substituting $\frac{dC_{mT}}{dt}$ from equation (3.39) we get from

Equation (3.48)

$$\frac{dJ_w}{dt} = K_w \frac{dJ_w}{dt} = K_w \left[\frac{d\Delta P}{dt} - \beta \frac{\dot{M}_{so} + b\dot{M}_{bo} + (1-p)\dot{M}_{po} - \dot{M}_{mm}}{F_{so}} \right] \quad (3.49)$$

3.3.2.3 Production of brine

The material balance for the production of brine or retentate is given by Sobana and Panda (2013) as

$$\frac{dm_{bT}}{dt} = F_{mm} - F_{bo} - F_{pi} - F_{co} \quad (3.50)$$

$$\frac{dC_{bT}}{dt} = \frac{\left[F_{mm}(C_{mm} - C_{bo}) - F_{pi}(C_{pi} - C_{bo}) - F_{co}(C_{co}) \right]}{V_{bT}} \quad (3.51)$$

The brine flow rate is given by

$$F_b = K_{bo} \sqrt{(P_{bi} - P_{bo})} \quad (3.52)$$

K_{bo} depends on valve characteristics. The above transient equations can be linearized around the operating point, from where the concentration dynamics is given by

$$C_{bT}(s) = \frac{F_{mm}}{sV_{bT} + F_{bo}} C_{mm}(s) - \frac{F_{pi}}{sV_{bT} + F_{bo}} C_{pi}(s) - \frac{F_{co}}{sV_{bT} + F_{bo}} C_{co}(s) \quad (3.53)$$

In the above equation, C represents the concentration, V represents the volume of the tank, F the volumetric flow rate, suffix b is for the brine, p stands for the permeate, i for the inlet and o for the outlet streams and suffix T for tank. The height of the liquid in the tank can be given as

$$h_{bT}(s) = \frac{C_{bi}R_{bT}/C_{bo}}{R_{bT}A_{bT}s+1} F_{bi}(s) \quad (3.54)$$

3.3.2.4 Product tank

After the solute comes out of the RO, it mixes with the streams of brine. The other stream, containing the solvent or permeate or product water gets accumulated / collected in the product tank at a rate F_p . A part of the product water flow may be withdrawn (F_w) as per demand, or it can also be recirculated (p part) to the feed tank. The continuity equation for the product tank becomes

$$[p]F_{po}C_{po} - F_{wo}C_{wo} = \frac{d}{dt}(V_{wT}C_{wT}) \quad (3.55)$$

where V_{wT} is the volume of the product water tank and C_{wT} is the concentration of the product water.

$$\frac{C_{pT}(s)}{C_{pi}(s)} = \frac{F_{mm} - F_{bi} - F_{co}}{sV_{pT} + (F_{mm} - F_{bi} - F_{co})} \quad (3.56)$$

and liquid height is given by

$$\frac{h_{pT}(s)}{F_{pi}(s)} = \frac{C_{pi}R_{pT}/C_{po}}{R_{pT}A_{pT}(s)+1} \quad (3.57)$$

The rate of change of mass can be balanced using mass flow rates as

$$\frac{dm_{pT}}{dt} = F_{pi} - F_{po} \quad (3.58)$$

Equations (3.46) and (3.58) are basically lumped equations representing concentration and the flow dynamics of the permeate.

3.3.2.5 Cake deposition module

Due to the transverse section of the flow, the solids get deposited on the walls of the membrane. As a result, layers of cake build up. After formulating the mass balance (Hyun-Jeoh et al.2009), and introducing the deviation variables, and finally taking the Laplace transform, we can get the following Equation.

$$M_c(s) = \frac{K_b}{s^2} [C_{bT}(s) - C_s(s)]^m \quad (3.59)$$

Where C_s is the salt saturation concentration.

$$K_b = K_c \psi S_p$$

and in this case, $m = 1$

The cake resistance is given by

$$\frac{R_c(t)}{m_c(t)} = \frac{\alpha}{A_m} \quad (3.60)$$

R_c is the cake resistance, m_c is the mass of the cake, α is the specific cake resistance and A_m is the area of the membrane module.

For $p=0$ and $b=0$, Eq(3.41) reduces to $C_{mT}(t) = \frac{C_{so}}{V_{mT}} \left[1 - e^{-t/\tau} \right]$

where $\tau = \frac{V_{mT}}{F_{mT}}$ at time $t=0$. The multivariable block diagram of the

integrated system (comprising of Feed tank, RO membranes & Product tank) can be constructed.

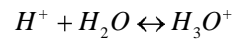
3.3.2.6 Pump module

The osmotic pressure exerted by the fluid is

$$\frac{\Delta P}{C_{mm}/C_{mT}} = 2RT \left(1 - \frac{C_{pT}}{C_{mm}} \right) C_{mT} \quad (3.61)$$

These mechanistic models (developed as above) are helpful in the steady state as well as in the transient simulation for model validation, and formulation of the linearized multi-input multi output models for controller synthesis.

3.3.2.7 pH model



The hydronium ion present in the water can be expressed as

$$H_3O = \sqrt{KC_a}$$

where K is the dissociation constant of the hydronium ions and C_a is their concentration. From the above expression the pH of the water is expressed as follows.

$$pH = -\log[H_3O]$$

Taking the Taylors approximation

$$pH = \log \left[\sqrt{K} * \sqrt{C_{ss}} + \left[\frac{\sqrt{K}}{2 * \sqrt{C_{ss}}} (C - C_{ss}) \right] \right] \quad (3.62)$$

The above pH model is used to find the pH for the feed, brine and permeate streams where K is the dissociation constant of the respective streams given by Kristin and George (2010). C is the concentration with suffix ss representing the steady state concentration of the respective streams.

3.4 RESULTS AND DISCUSSION

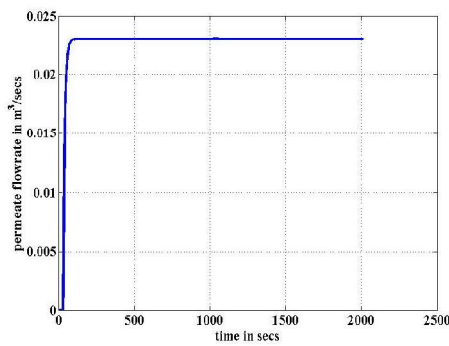
3.4.1 Parametric Studies (Effect of change in Parameters on the performance)

In this section, the theoretical model is simulated and the output is obtained. When the plant runs under the steady operating condition, the permeate flow is calculated for different values of pump pressures. These calculated values are compared with those obtained experimentally. Table 3.1 shows the nominal operating conditions of the RO Process

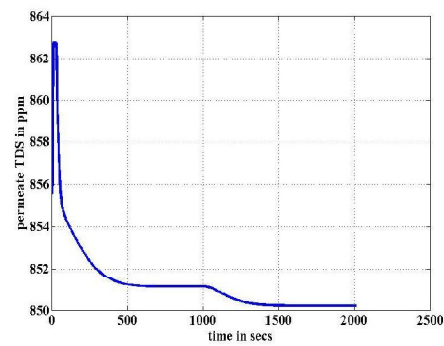
Table 3. 1 The nominal operating conditions of the plant

Serial No	Variables	Value
1.	Concentration of feed in the mixing tank	40000 ppm
2.	Concentration of feed to the RO module	41350 ppm
3.	Flowrate of feed to the RO module	180 m ³ /hr
4.	Volume of feed water	4.4944m ³
5.	Flow rate of mixed feed water	180 m ³ /hr
6.	Permeate (due to vertical component of velocity) comes out along the surface of the membrane. The value is 1 if the permeate is recycled	0
7.	Concentrated brine (due to horizontal component of velocity) flows axially through the membrane. The value is 1 if the brine is recycled	0.725
8.	Concentration of the permeate from the RO module	850 ppm
9..	Flow rate of the permeate from the RO module	80 m ³ /hr
10.	Concentration of brine from the RO module	60000 ppm
11.	Flow rate of brine from the RO module	90 m ³ /hr

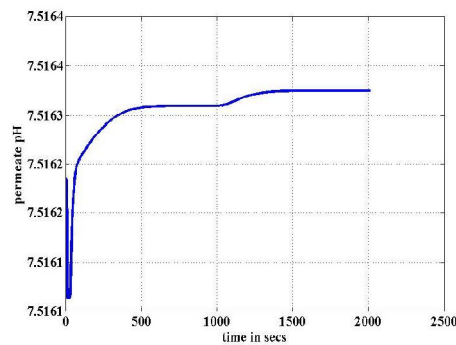
Similarly, if the pump pressure get settled (from 1 bar to 60 bar) and a 10% change in feed flow is given and the responses of the permeate flow rate & concentration of permeate and that of brine are observed from the computation of the model equations. The transient behaviours are as shown in Figure 3.2.



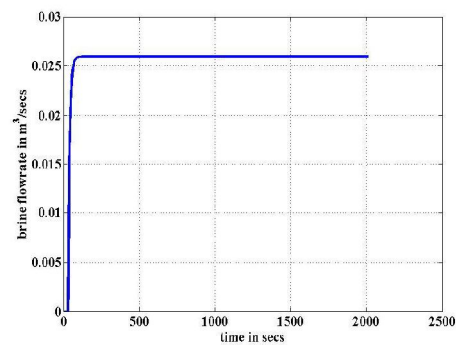
(a).Time profile of the permeate flow-rate



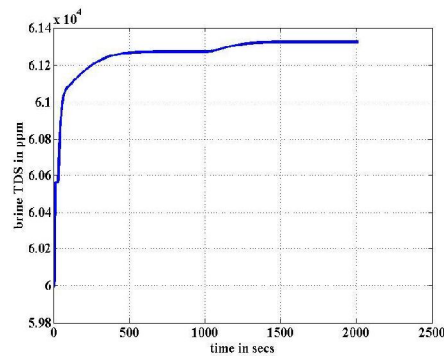
(b).Time profile of the permeate concentration



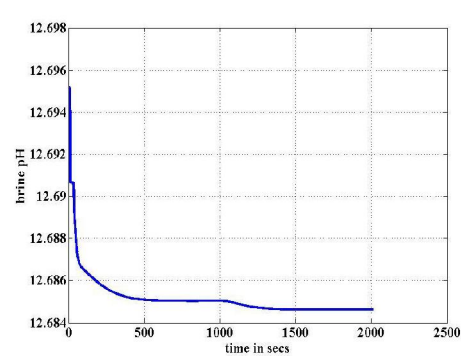
(c).Time profile of the permeate pH



(d).Time profile of the brine flowrate.



(e).Time profile of the brine Concentration



(f). Time profile of the brine pH

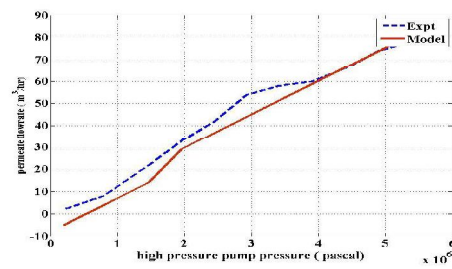
Figure 3.2 Step responses of streams (0-1000 s) for a step change of 10% (after 1000 s) in the feed-flow rate of the raw feed. [for permeate stream (a) flowrate, (b) concentration and (c) pH; for brine stream (d) flowrate, (e) concentration (f) pH]

3.4.2 Model Validation

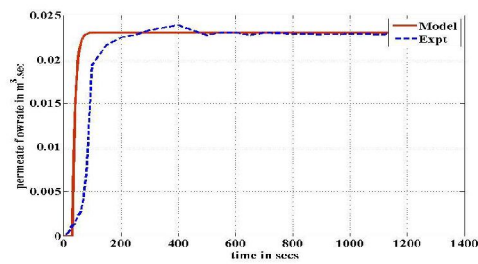
The theoretical response is obtained after simulating the model as per Figure 3.1. The computed responses are plotted along with experimental data in Figure 3.3. The mathematical models are validated in two different modes. (i) the steady state (Figure 3.3.a) and the (ii) transient / start up mode. When the plant ran at a steady state, pump pressure data was collected. These are treated as input data to the RO module. Using these data, the output (flow rate) from the RO is calculated using equation J_w in RO section. These calculated outputs are plotted (Figure 3.3.a) against pump pressure, and are compared with the same (measured flowrate from the exit of RO) against the pump inputs. The calculated error between the two curves is found to be 0.5041. When the plant was in the startup mode, pump pressure data (input) are collected, and the outputs (flow rate, concentration and pH) from the exit of the permeate tank (as described in Figure 3.3.b,c,d) and ((flow rate, concentration and pH) from the exit of the brine tank (as described in Figure 3.3.e,f,g) are recorded. The same variables (flow rate and concentration from the permeate tank) from the model equations are calculated after simulating (a step input of 60 bar is provided as ΔP of pump to calculate the outputs from the permeate tank) the developed model. The recorded (experimental) and theoretically calculated values (simulated) are compared in Figure 3.3.b and 3.3.c. It is found that both the responses are in close agreement as discussed in the result and discussion section of Table 3.2 (and

$$\text{the MSE } e = \sum_{i=1}^n \left(\frac{y_{m_i} - y_{e_i}}{n} \right)^2 \text{ with } y_m \text{ as measured and } y_e \text{ as estimated values,}$$

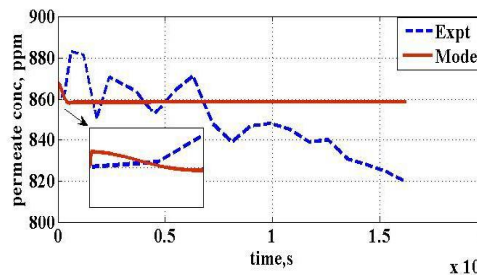
calculated between the curves are 4.2893 (Figure 3.3.b), 3.3281 (Figure 3.3.c) 7.868 (Figure 3.3.d) 1×10^{-8} (Figure 3.3.e), 1×10^{-8} (Figure 3.3.f) and 3.422 (Figure 3.3g) respectively.



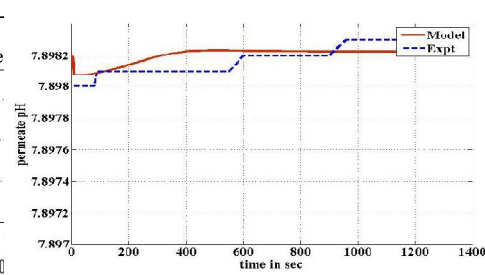
(a) pump pressure vs permeate flowrate



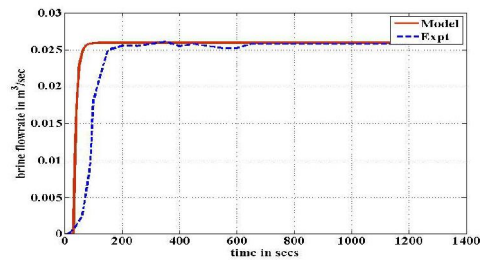
(b) permeate flowrate vs time



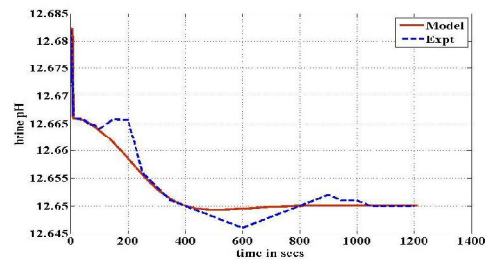
(c) permeate TDS vs time



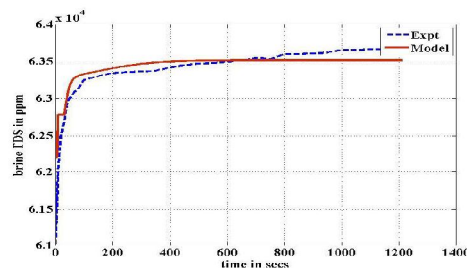
(d) permeate pH vs time



(e) brine flow vs time



(f) brine pH vs time



(g).brine TDS vs time

Figure 3.3 Comparison of step responses of flow rate, concentration and pH of permeate as well as of brine with respect to the theoretical (model) and experimental values [showing validation of the model with experimental values: the steady state result is in (a) and the unsteady state results are in (b), (c), (d), (e), (f) and (g)]

Equation (3.31) can be used to find the concentration of the permeate. Figure 3.4 shows the concentration profiles (Eqn.3.46) along the radius of the RO. Streams at the centre of the RO contain the initial concentration, C_{f0} which is plotted in the y axis. The concentration declines as the radial length increases from the centre of the membrane. With different values of C_{f0} the concentrations profiles are plotted in Figure 3.4. The horizontal axis of Figure 3.4 is made as radial length(y). In Equation (3.46), x means axial length. Using numerical methods the concentration of feed comes down as the feed water passes through the RO module from the outer radius of RO to the inner radius of RO at different position from the entry to the exit.

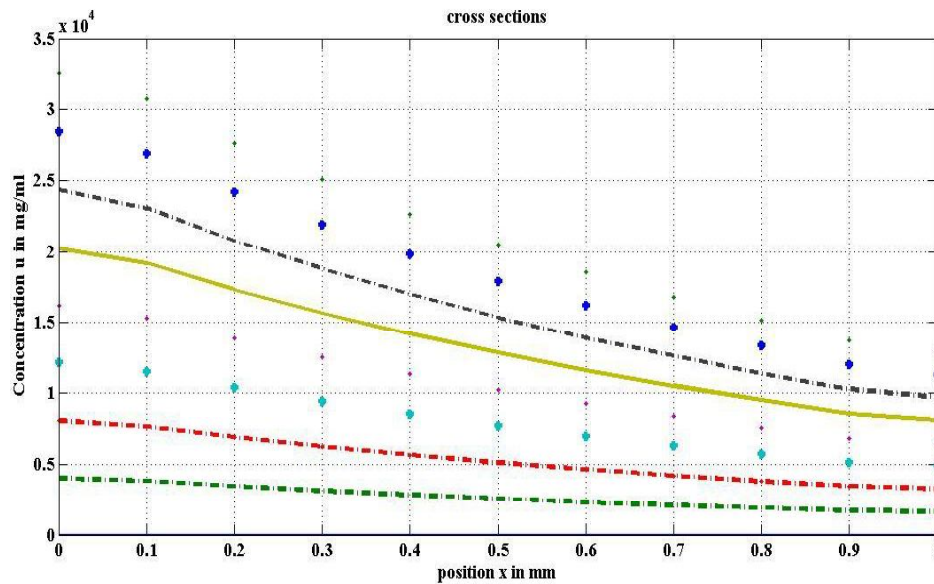


Figure 3.4 Concentration profiles along the radial length of the RO membranes with different initial concentrations

Equations (3.35-3.52) are solved in MATLAB and the transient responses of the flow rate, and the concentration at the exit of the RO module and the potable water tank and brine are plotted (Figure 3.5) for step disturbance in the feed streams of the respective units. The steady state

results of the permeate flow-rate (F_p) for various values of the feed-flow rate are computed, using the present model and compared with the same from Chen-Jen Lee et al. (2010). It is found that the results from the present study are in close agreement with those of Chen-Jen Lee et al. (2010); thus, the model has been validated. It can be seen (Figure 3.5) that the permeate flow-rates from Chen et al. behave linearly with the feed flow rate; while those from the present model show a little non-linearity, establishing the fact that the permeate flow rate changes with the feed flow-rate nonlinearly. Moreover, the recovery calculated from Chen-Jen Lee et al. (2010) is 40%, whereas it is 44% as obtained from the present model.

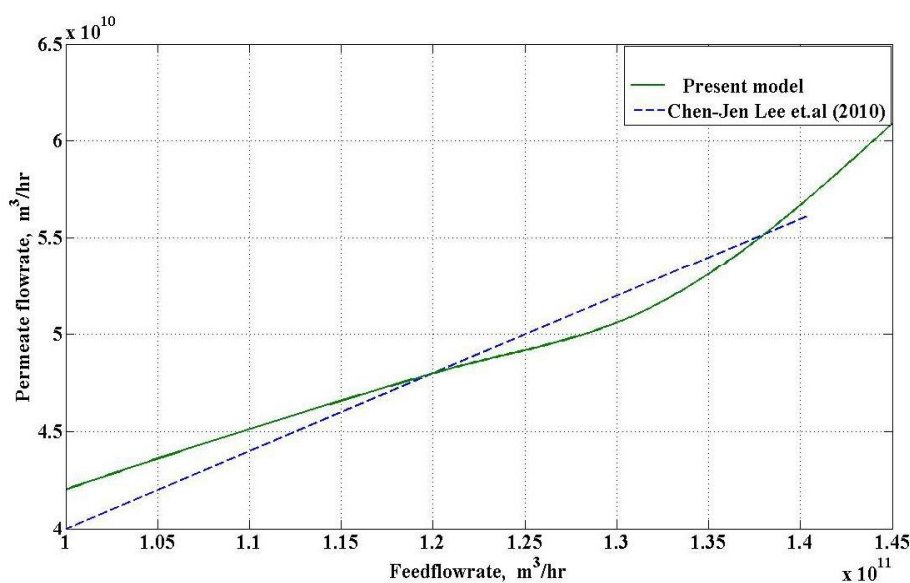


Figure 3.5 Comparison of the computed permeate flow-rates for different feed flow-rates using the present model and that of by Chen Jen Lee et al (2010).

3.4.3 Linearized Model

Thus the desalination system developed here, has two manipulated inputs and three measured outputs. The inputs to the multivariable system are

the pump pressure (ΔP), and ratio (R_{FB}) of the flow rates of sea water feed to that of the total feed stream (recycle + sea water) as it enters the equalization tank (as shown in Figure 3.1), then substitute ΔP and R_{FB} in simulink to simulate the model. The outputs to the multi input multi output system are permeate concentration, flow rate and pH. The transfer function of the developed model is given by Equation (3.63)

$$\begin{bmatrix} F_p \\ C_p \\ pH_p \end{bmatrix} = \begin{bmatrix} \frac{1.4944e^{-0.55s}}{0.71615s+1} & \frac{0.092857e^{-0.3666s}}{1.1875s+1} \\ \frac{-0.51e^{-0.55s}}{0.717834s+1} & \frac{-16.0482e^{-0.2333s}}{3.31s+1} \\ \frac{0.114411e^{-0.55s}}{7s+1} & \frac{0.178e^{-0.15s}}{2.5s+1} \end{bmatrix} \begin{bmatrix} \Delta P \\ R_{FB} \end{bmatrix} \quad (3.63)$$

The R^2 values of the models (calculated between graphs from theoretical model and experimental graph) given in Figure 3.3 are listed in Table 3.2 below. Regression is estimated using statistical means and least square procedure. The open loop MIMO (2x3) linearized nonsquare RO process model is shown in Figure 3.6.

Table 3.2 Values of R^2 between the theoretical models and experimental data

R^2 value for permeate flowrate	R^2 value for pump pressure vs permeate flowrate	R^2 value for brine flowrate	R^2 value for permeate concentration	R^2 value for permeate pH	R^2 value for brine pH
0.9293	0.9795	0.9962	0.9795	0.9722	0.9734

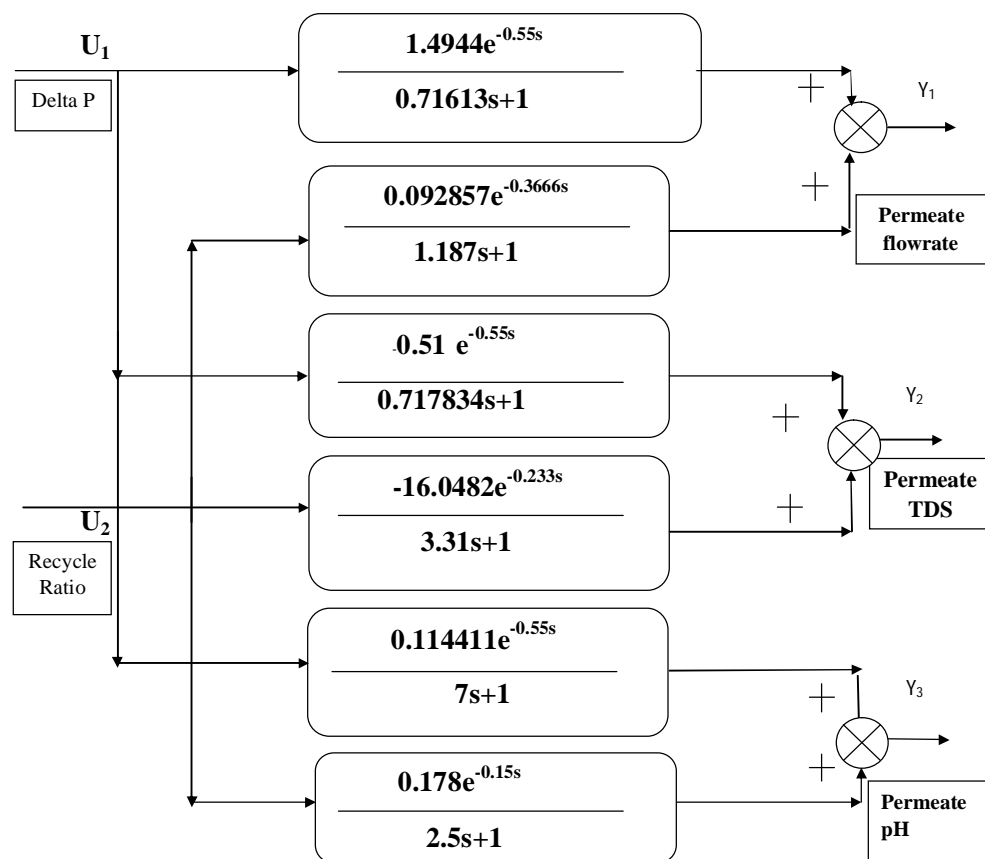


Figure 3.6 Multi input and multi output RO process model

3.5 SUMMARY

A comprehensive mechanistic mathematical model representing the individual units of the desalination process is formulated from the first principles of mass transfer. The integrated system is of the multivariable type in nature and is represented as having two inputs, namely, pump pressure and ratio of the flow rates of sea water feed to that of the brine stream; and three outputs, namely, permeate concentration, flow rate and pH. The steady state and transient behaviour of the model are validated using practical industrial data. Permeate flow rates are calculated from the steady state model equations for different values of pump pressures to validate the steady state behaviour of the process by comparing similar industrial data obtained practically. Similarly, the flow rates and concentrations of the permeate stream are calculated for the step changes in inputs using the transient model, and are validated using similar recorded data from the experiments. Thus, the developed model has been validated. The linearized model is useful for further study for safe operation and control of the process. This reliable RO model is of great importance for process design, operation and control.